ARTICLES
https://doi.org/10.1038/s41551-020-00613-9

nature biomedical engineering

Extensive germline genome engineering in pigs

Yanan Yue[1,8], Weihong Xu[1,8], Yinan Kan[2,8], Hong-Ye Zhao[3,8], Yixuan Zhou[1,8], Xiaobin Song[1,8], Jiajia Wu[1], Juan Xiong[1], Dharmendra Goswami[2], Meng Yang[1], Lydia Lamriben[2], Mengyuan Xu[1], Qi Zhang[1], Yu Luo[1], Jianxiong Guo[3], Shengyi Mao[3], Deling Jiao[3], Tien Dat Nguyen[3], Zhuo Li[3], Jacob V. Layer[2], Mailin Li[2], Violette Paragas[2], Michele E. Youd[2], Zhongquan Sun[4], Yuan Ding[4], Weilin Wang[4], Hongwei Dou[1], Lingling Song[1], Xueqiong Wang[1], Lei Le[1], Xin Fang[1], Haydy George[2], Ranjith Anand[2], Shi Yun Wang[2], William F. Westlin[2], Marc Güell[5], James Markmann[6], Wenning Qin[2,9], Yangbin Gao[1,9], Hong-Jiang Wei[3,9], George M. Church[7,9] and Luhan Yang[1,9] ✉

The clinical applicability of porcine xenotransplantation—a long-investigated alternative to the scarce availability of human organs for patients with organ failure—is limited by molecular incompatibilities between the immune systems of pigs and humans as well as by the risk of transmitting porcine endogenous retroviruses (PERVs). We recently showed the production of pigs with genomically inactivated PERVs. Here, using a combination of CRISPR–Cas9 and transposon technologies, we show that pigs with all PERVs inactivated can also be genetically engineered to eliminate three xenoantigens and to express nine human transgenes that enhance the pigs' immunological compatibility and blood-coagulation compatibility with humans. The engineered pigs exhibit normal physiology, fertility and germline transmission of the 13 genes and 42 alleles edited. Using in vitro assays, we show that cells from the engineered pigs are resistant to human humoral rejection, cell-mediated damage and pathogenesis associated with dysregulated coagulation. The extensive genome engineering of pigs for greater compatibility with the human immune system may eventually enable safe and effective porcine xenotransplantation.

The limited availability of organs for human transplantation is a serious unmet medical need[1]. Owing to their similar organ sizes and physiology to humans, pigs have long been thought to be a promising source of organs for human transplantation. However, safe and effective xenotransplantation has been impeded by two major hurdles: (1) immunological and physiological molecular incompatibilities between the porcine graft and the human recipient and (2) the risk of cross-species transmission of porcine endogenous retroviruses (PERVs)[1–5].

PERVs can infect human cells in vitro, propagate among human cells and recombine to adapt to the human host, posing a zoonosis concern[4,6]. As PERV sequences are part of the porcine genome, they cannot be eliminated by bio-secure breeding, which can be performed for other zoonotic pathogens. We have previously demonstrated genome-wide inactivation of all copies of the PERV reverse transcriptase *pol* using CRISPR–Cas9, successfully producing PERVKO pigs and eliminating the potential risk of viral transmission[6].

The other major barrier of xenotransplantation is organ rejection due to molecular incompatibilities between pig organs and the human immune system. In particular, some porcine-specific glycan epitopes, primarily galactose-alpha-1,3-galactose (α-Gal), *N*-glycolylneuraminic acid (Neu5Gc) and the SDa epitope, can be recognized by preformed antibodies in the human serum. The binding of preformed antibodies to these epitopes initiates hyperacute rejection (HAR) through activation of the complement cascade[7–9]. Genetic inactivation of *GGTA1* (encoding alpha-1,3-galactosyltransferase), *CMAH* (encoding cytidine monophosphate-*N*-acetylneuraminic acid hydroxylase) and *B4GALNT2* (encoding beta-1,4-*N*-acetyl-galactosaminyltransferase 2) removes α-Gal, Neu5Gc and the SDa epitopes (hereafter 3KO), respectively, which has been proven to substantially decrease human preformed antibody binding in vitro[10–13]. Encouragingly, xenografts from *GGTA1*-knockout (GTKO) pigs have already been shown to reduce HAR and prolong graft survival in non-human primate (NHP) models[14,15]. Moreover, overexpression of human complement regulatory proteins (CRPs)—including CD46 (membrane cofactor protein), CD55 (decay-accelerating factor) and CD59 (MAC-inhibitory protein)—has been shown to attenuate HAR and prolong graft survival[16–18]. Furthermore, to address the infiltration of natural killer (NK) cells and macrophages into xenograft organs[19], previous studies have also tried to (1) reduce NK-cell-mediated toxicity by inhibitory signalling through the overexpression of human B2M–HLA-E fusion protein in porcine endothelial cells[20] and (2) reduce macrophage-mediated toxicity by CD47–SIRPα signalling through the expression of human CD47 (ref. [21]).

Furthermore, the incompatibility between the pig and human coagulation systems may lead to thrombotic microangiopathy and systemic consumptive coagulopathy, as observed in many xenotransplantation preclinical experiments[2]. In particular, porcine thrombomodulin (THBD) is incapable of binding to human thrombin to activate antithrombotic protein C and prevent clot formation[22].

[1]Qihan Bio Inc, Hangzhou, China. [2]eGenesis Inc, Cambridge, MA, USA. [3]Key Laboratory of Animal Gene Editing and Animal Cloning in Yunnan Province, Yunnan Agricultural University, Kunming, China. [4]Department of Hepatobiliary and Pancreatic Surgery, The Second Affiliated Hospital, Zhejiang University School of Medicine, Hangzhou, China. [5]Department of Experimental and Health Sciences, Pompeu Fabra University, Barcelona, Spain. [6]Department of Surgery, Massachusetts General Hospital, Boston, MA, USA. [7]Department of Genetics, Harvard Medical School, Boston, MA, USA. [8]These authors contributed equally: Yanan Yue, Weihong Xu, Yinan Kan, Hong-Ye Zhao, Yixuan Zhou, Xiaobin Song. [9]These authors jointly supervised this work: Wenning Qin, Yangbin Gao, Hong-Jiang Wei, George M. Church, Luhan Yang. ✉e-mail: luhan.yang@qihanbio.com

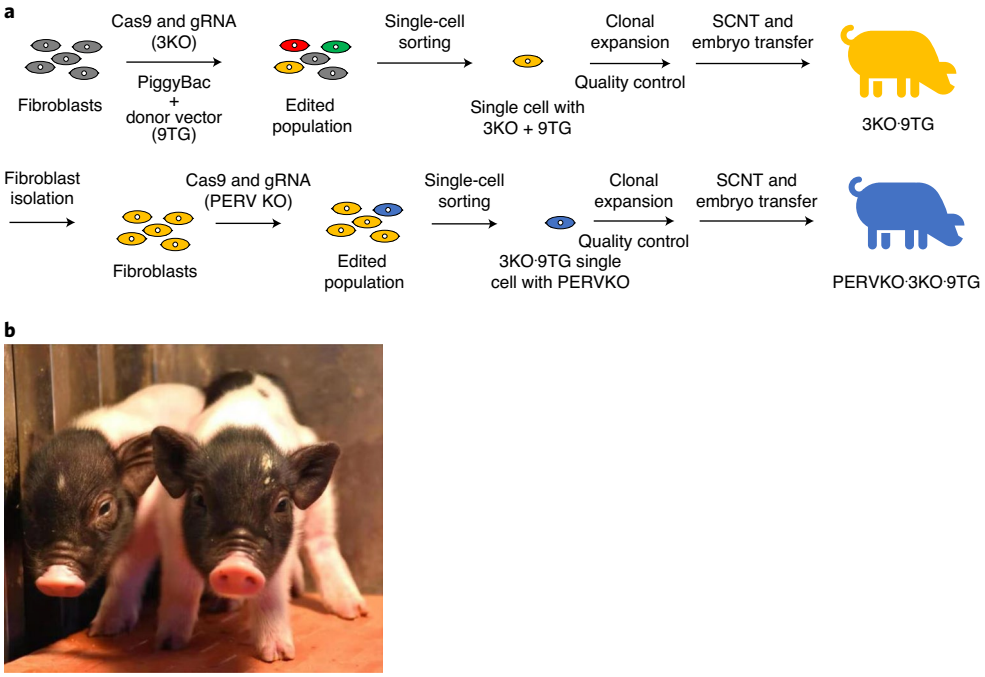

Fig. 1 | The engineering of PERVKO·3KO·9TG pigs. a, The workflow to generate PERVKO·3KO·9TG pigs. WT Bama ear fibroblasts were edited using a mixture of Cas9 protein, gRNAs targeting *GGTA1*, *CMAH* and *B4GALNT2*, a donor vector carrying the expression cassettes for 9TG (h*CD46*, h*CD55*, h*CD59*, h*THBD*, h*TFPI*, h*CD39*, h*B2M*, *HLA-E* and h*CD47*) and a vector encoding PiggyBac transposase (PiggyBac). The edited population was sorted into single-cell clones carrying knockout of *GGTA1*, *CMAH* and *B4GALNT2* and 9TG integration. The selected cells were cloned into 3KO·9TG pigs using SCNT. In the next round of engineering, fibroblasts from 3KO·9TG pigs were isolated and further edited to inactivate PERVs using Cas9 and gRNAs targeting the *pol* gene of PERVs. The edited 3KO·9TG cells were single-cell sorted for clones carrying PERVKO in addition to 3KO and 9TG, and cloned into PERVKO·3KO·9TG pigs. **b**, An image of PERVKO·3KO·9TG piglets.

Moreover, although the degree of incompatibility between pig and human tissue factor pathway inhibitor (TFPI) has yet to be fully elucidated[23,24], some studies have shown that porcine TFPI does not effectively inhibit the human factor Xa and VIIa–tissue factor (TF) complex to prevent thrombin formation[25–27]. Beyond that, porcine CD39 is inactivated after endothelial cell activation, and its expression is insufficient to inhibit human platelet aggregation[25,28]. To minimize this incompatibility, several genetic modifications targeting the coagulation pathways have been tested and proven to be effective[29–31].

To date, more than 40 genetic modifications have been attempted, either individually or in combination, in pigs with the goal to mitigate incompatibility[16,32–35]. Encouragingly, pigs carrying triple knockouts of *GGTA1*, *CMAH* and *B4GALNT2* have been reported to achieve a significant reduction in human preformed antibody binding[13,16]. Furthermore, various human transgenes have demonstrated beneficial outcomes in preclinical models[36]. In particular, one recent study showed that the cardiac xenograft from a pig carrying knockout of *GGTA1* and overexpression of h*CD46* and h*THBD* achieved life-supporting function in baboons for 6 months[37]. Another study showed that a rhesus macaque monkey lived for more than 400 d with the renal xenograft from a pig carrying knockout of *GGTA1* and overexpression of h*CD55* (ref. [38]). These studies support that long-term graft survival is achievable using genetically engineered xenograft organs.

Despite years of efforts, no pig organs have been engineered with the combined features of PERV inactivation and improved immunological and coagulation compatibility, which is ideal for clinical applications[16]. Here we sought to use advanced genome-modification tools and cloning technology to create clinically relevant pig organs for xenotransplantation.

Results

First, we engineered 3KO·9TG pigs carrying 3KO to eliminate major xenoantigens and nine human transgenes (9TG) to enhance the immunological and coagulation compatibility between pigs and humans. Next, we inactivated all PERVs from the 3KO·9TG pig genome to produce PERVKO·3KO·9TG pigs carrying 3KO, 9TG and PERVKO (Fig. 1).

To engineer 3KO·9TG pigs, we electroporated wild-type (WT) porcine ear fibroblasts with CRISPR–Cas9 reagents targeting *GGTA1*, *CMAH* and *B4GALNT2*, a plasmid encoding PiggyBac transposase[39], and a transposon construct carrying nine human transgenes (h*CD46*, h*CD55*, h*CD59*, h*B2M*, *HLA-E*, h*CD47*, h*THBD*, h*TFPI* and h*CD39*; Figs. 1a and 2a, Supplementary Note 1 and Methods). We next isolated and expanded single-cell clones, and (1) screened for clones carrying the desired frameshift mutations on the 3KO genes using Sanger sequencing and (2) screened for the presence of 9TG using PCR (Fig. 2). After obtaining the modified cells, we validated the genotype using whole-genome sequencing (WGS). We performed somatic cell nuclear transfer (SCNT) using the validated clones and successfully produced 3KO·9TG pigs.

To generate PERVKO·3KO·9TG pigs, we electroporated 3KO·9TG pig fibroblasts with CRISPR–Cas9 reagents targeting the *pol* gene common to all 25 copies of the PERV elements[6]. We next screened and selected for single-cell clones carrying exclusively large deletions encompassing the catalytic core of the *pol* gene, as determined using deep sequencing (Supplementary Fig. 1). Finally, we selected the set of clones on the basis of the presentation of a normal karyotype and, with these clones, we successfully produced PERVKO·3KO·9TG pigs using SCNT (Supplementary Fig. 2 and Fig. 1b). We did not observe any abnormality in the cloning efficiency of PERVKO·3KO·9TG pigs (Supplementary Note 2).

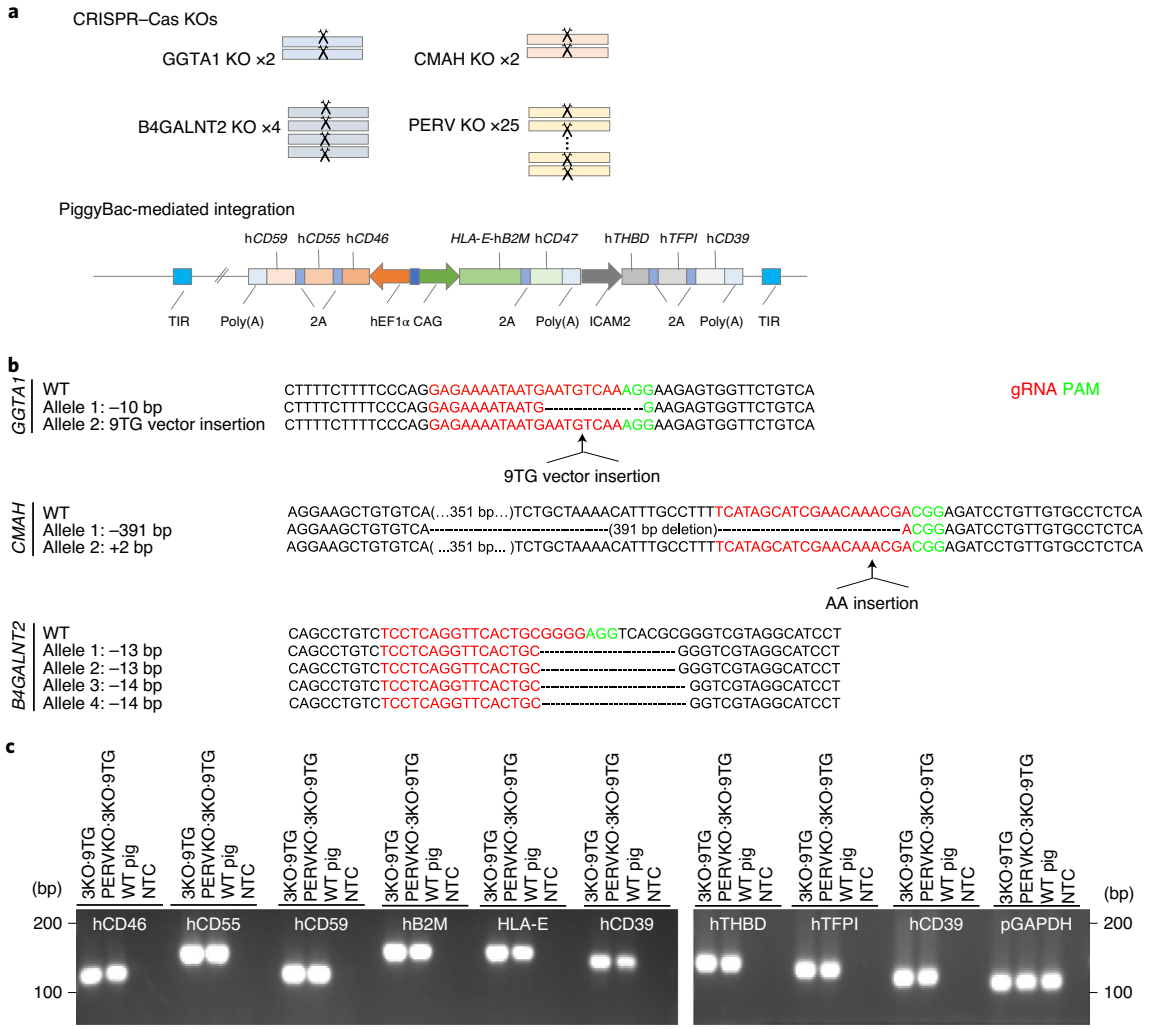

Fig. 2 | PERVKO·3KO·9TG pig engineering and validation of the 3KO and 9TG edits at the genomic level. a, Schematic of the 42 modified alleles. We generated the 3KO and PERVKO edits using CRISPR–Cas9 with gRNAs targeting the 2 copies of *GGTA1*, 2 copies of *CMAH*, 4 copies of *B4GALNT2* and 25 copies of the PERV element. We generated 9TG using PiggyBac-mediated random integration of the nine human transgenes into the pig genome. The transgenes are expressed from three transcription cassettes, with each cassette expressing two to three genes linked by the porcine teschovirus 2A (2A) peptide. TIR, terminal inverted repeats of the PiggyBac transposon; hEF1α, CAG and ICAM2, promoters; Poly(A), polyadenylation signal. **b**, WGS confirmation of the frameshift mutations of *GGTA1*, *CMAH* and *B4GALNT2* in 3KO·9TG pigs and PERVKO·3KO·9TG pigs. AA insertion, an insertion of two adenosines. **c**, Agarose gel image of PCR products, confirming the presence of the nine human transgenes in the 3KO·9TG and PERVKO·3KO·9TG fetal fibroblasts, and their absence in the WT fetal fibroblasts and no-template controls (NTC). A list of the primers used is provided in Supplementary Table 1. Experiments were independently repeated three times with similar results obtained.

We next sought to examine the on-target and off-target effects of genetic modifications in PERVKO·3KO·9TG pigs. To this end, we performed linked-reads WGS of WT, 3KO·9TG and PERVKO·3KO·9TG ear fibroblasts. Consistent with our deep-sequencing data, we confirmed that mutations introduced into the 25 copies of the PERV element and 8 alleles of the 3KO genes were frameshift insertions or deletions (Supplementary Fig. 1 and Fig. 2b). We did not observe any difference in structural variants between WT and 3KO·9TG pigs, or between 3KO·9TG pigs and PERVKO·3KO·9TG pigs, indicating that the genome of these engineered pigs was largely stable. For the small indels, we examined all 1,211 predicted off-target sites and found two small insertions in the *B4GALNT2* guide RNA (gRNA) off-target sites in 3KO·9TG pigs compared with the WT. However, neither of these insertions affected the protein-coding sequence (Supplementary Fig. 3). Comparing the PERVKO·3KO·9TG genome and the 3KO·9TG genome, we also found two deletions and one insertion in the predicted PERV gRNA off-target sites (Supplementary Fig. 3). None of these were located within any annotated protein-coding region. Notably, we could not rule out the possibility that these mutations could be derived from spontaneous somatic mutations[40,41]. In view of the lack of functional implications and the normal in vivo pathophysiological data of engineered pigs (Supplementary Fig. 4), we concluded that the germline-engineered PERVKO·3KO·9TG pigs maintained genomic stability.

Having confirmed the genomic modifications at the DNA level, we further examined whether PERVKO·3KO·9TG pigs have the correct 3KO and 9TG expression. We first performed RNA sequencing (RNA-seq) analysis of fibroblasts and endothelial cells and found that both 3KO·9TG pigs and PERVKO·3KO·9TG pigs expressed all of the transgenes at levels comparable to or higher than the expression levels in human umbilical vein endothelial cells (HUVECs; Fig. 3a). We also observed consistent transgene expression across different cell types (porcine umbilical vein endothelial

cells (PUVECs) and fibroblasts) and tissues (heart, kidneys, liver and lungs; Supplementary Fig. 5a), suggesting that the transgenes are ubiquitously expressed in vivo. We next characterized protein expression in the engineered pigs. We observed a decrease in glycan markers of α-Gal, Neu5Gc and SDa on endothelial cells, as well as in heart and kidney tissues, suggesting that the three genes responsible for synthesizing these glycan epitopes in both 3KO·9TG pigs and PERVKO·3KO·9TG pigs were functionally eliminated (Fig. 3b,c and Supplementary Fig. 6). Using fluorescence-activated cell sorting (FACS) analysis of PUVECs, we observed that both 3KO·9TG pigs and PERVKO·3KO·9TG pigs expressed all of the transgenes at the protein level. Eight out of the nine transgenes were robustly expressed at levels comparable to HUVECs, which we further confirmed at the protein level in multiple tissues (Fig. 3c and Supplementary Figs. 6 and 7). We confirmed that the constitutive protein expression of transgenes (hCD46, hCD55, hCD59 and hCD39) was achieved in endothelial cells and different tissues (heart, kidneys, liver and lungs; Supplementary Fig. 7) using western blot analysis. Expression of hB2M, HLA-E, hCD47 and hTFPI was detected in both kidney and heart tissues using immunofluorescence staining (Fig. 3c and Supplementary Fig. 6). Interestingly, THBD expression was detected using RNA-seq and FACS, but not at detectable levels using immunofluorescence or western blot analysis. Taken together, we concluded that our 3KO and 9TG genetic modifications largely translated into successful RNA and protein expression at the cellular and tissue level in the engineered pigs.

To assess the overall health of our engineered pigs, we examined their physiology and fertility and the transmissibility of the genetic modifications to their offspring. We observed that both PERVKO pigs and 3KO·9TG pigs, although having been extensively engineered, demonstrated normal blood cell counts, including total white blood cell, platelet, monocyte and neutrophil counts (Supplementary Fig. 4a). According to blood tests, we also observed normal vital organ functions in the liver, heart and kidneys of our engineered pigs (Supplementary Fig. 4b–d). Moreover, our engineered pigs had similar prothrombin and thrombin time as compared with WT pigs (Supplementary Fig. 4e), indicating normal coagulation function.

Furthermore, we found that PERVKO and 3KO·9TG pigs were fertile, with an average litter size of seven. Offspring bred from PERVKO pigs with WT pigs carry ~50% PERV inactivated alleles in their liver, kidney and heart tissues, indicating that the knockout alleles are stably inherited (Supplementary Fig. 8). Similarly, all offspring of 3KO·9TG pigs and WT pigs are heterozygous for 3KO, and about half of them carry 9TG (Supplementary Fig. 9a). The expression levels were validated at both the mRNA (Supplementary Fig. 9b) and protein (Supplementary Fig. 9c) levels. This suggests that the genetic modifications are stable and expressed in the F_1 generation. We therefore concluded that the engineered PERVKO pigs and 3KO·9TG pigs exhibit normal physiology, fertility and germline transmission of the edited alleles.

We next examined whether our genetically modified pigs acquired novel functions as designed. We first tested whether the genetic modifications enabled the modified pig cells to evade preformed human antibody binding. Compared with WT PUVECs, 3KO·9TG PUVECs and PERVKO·3KO·9TG PUVECs both showed about 90% reduction in antibody binding to human IgG and IgM, confirming that the antibody barrier to xenotransplantation can be greatly mitigated by 3KO (Fig. 4a–c). Moreover, when incubated with a uniform pool of human serum complement, PERVKO·3KO·9TG PUVECs demonstrated minimal in vitro human complement cytotoxicity similar to their HUVEC counterparts (Fig. 4d), indicating the potential benefit of expressing human CRP transgenes (h*CD46*, h*CD55* and h*CD59*) in donor organs. To confirm whether each human CRP transgene can attenuate complement cytotoxicity, we expressed h*CD46*, h*CD55* and h*CD59* separately in WT porcine ear fibroblasts (Supplementary Fig. 10). Indeed, compared with controls, all porcine fibroblasts expressing any of h*CD46*, h*CD55* and h*CD59* significantly reduced complement-dependent cytotoxicity, demonstrating the proper function of each transgene in vitro.

We next examined whether PERVKO·3KO·9TG pigs are more resistant to human innate cellular immunity-mediated damage. Consistent with previous reports[20,42], compared with WT PUVECs, PERVKO·3KO·9TG PUVECs expressing human B2M and HLA-E fusion protein showed significantly higher resistance to NK-cell-mediated cell killing (Fig. 4e). Furthermore, PERVKO·3KO·9TG pigs expressing h*CD47* revealed significantly reduced phagocytosis by human macrophages in vitro, potentially through the CD47–SIRPα signalling pathway[21] (Fig. 4f). Taken together, these results suggest that our PERVKO·3KO·9TG pig xenograft was successfully engineered and may be more resistant to attack from the human innate cellular immunity.

Finally, we examined whether PERVKO·3KO·9TG pigs can attenuate the dysregulated activation of platelets and coagulation cascades. When vascularized WT porcine organs are transplanted, preformed human antibodies, complement and innate immune cells induce endothelial cell activation and trigger coagulation and inflammation[2]. The incompatibility between porcine coagulation regulatory factors and human blood can lead to abnormal platelet activation and thrombin formation[2,25], exacerbating the damage. To address this issue, we overexpressed h*CD39* in PERVKO·3KO·9TG pigs. The ADPase function of CD39 hydrolyses ADP (a potent platelet antagonist), thereby inhibiting human platelet activation. Analysis using an in vitro ADPase biochemical assay showed that, compared with WT PUVECs and HUVECs, CD39 activity in PERVKO·3KO·9TG PUVECs was significantly higher, which was consistent with its higher mRNA and protein expression (Supplementary Fig. 11). Moreover, molecular incompatibilities of coagulation regulators (such as TFPI) between pigs and humans render the extrinsic coagulation regulation ineffective. To address this issue, we overexpressed hTFPI in PERVKO·3KO·9TG pigs[43]. As expected, activated PERVKO·3KO·9TG PUVECs effectively bind to and neutralize human Xa, which mitigates coagulation and reduces the formation of thrombin–antithrombin (TAT) complexes (Supplementary Fig. 12). To examine coagulation reaction holistically, we cocultured human whole blood with PERVKO·3KO·9TG PUVECs and found minimal non-specific TAT formation, similar to that of HUVECs (Fig. 4g), suggesting that PERVKO·3KO·9TG pigs acquired enhanced coagulation compatibility with human factors.

Collectively, our results indicate that cells from PERVKO·3KO·9TG pigs acquired enhanced compatibility with the human immune

Fig. 3 | Validation of 3KO and 9TG in 3KO·9TG pigs and PERVKO·3KO·9TG pigs at the mRNA and protein levels. a, Heat map of transgene expression measured using RNA-seq in PUVECs and fetal/ear fibroblasts of WT, 3KO·9TG and PERVKO·3KO·9TG pigs. WT HUVECs were included as a comparison. Each row represents one transgene and each column represents one sample. Expression level is colour coded in blue, yellow and red, representing low, medium and high, respectively. The colour scale indicates the sample type. **b**,**c**, FACS validation of 3KO (**b**) and 9TG (**c**) in 3KO·9TG PUVECs, PERVKO·3KO·9TG PUVECs, HUVECs and WT pigs. The gating strategy is shown in Supplementary Fig. 15. **d**, Immunofluorescence staining validation of 3KO and 9TG in 3KO·9TG and PERVKO·3KO·9TG kidney cryosections. A list of the antibodies used is provided in Supplementary Table 2. Scale bars, 75 μm. Experiments were independently repeated twice with similar results obtained for **b** and **c**.

system through attenuated human antibody binding, complement toxicity, NK cell toxicity and macrophage phagocytosis, as well as through restored coagulation regulation.

Discussion

Genetically engineered pigs hold great promise in meeting the unmet medical need for human transplantable organs. Here we used

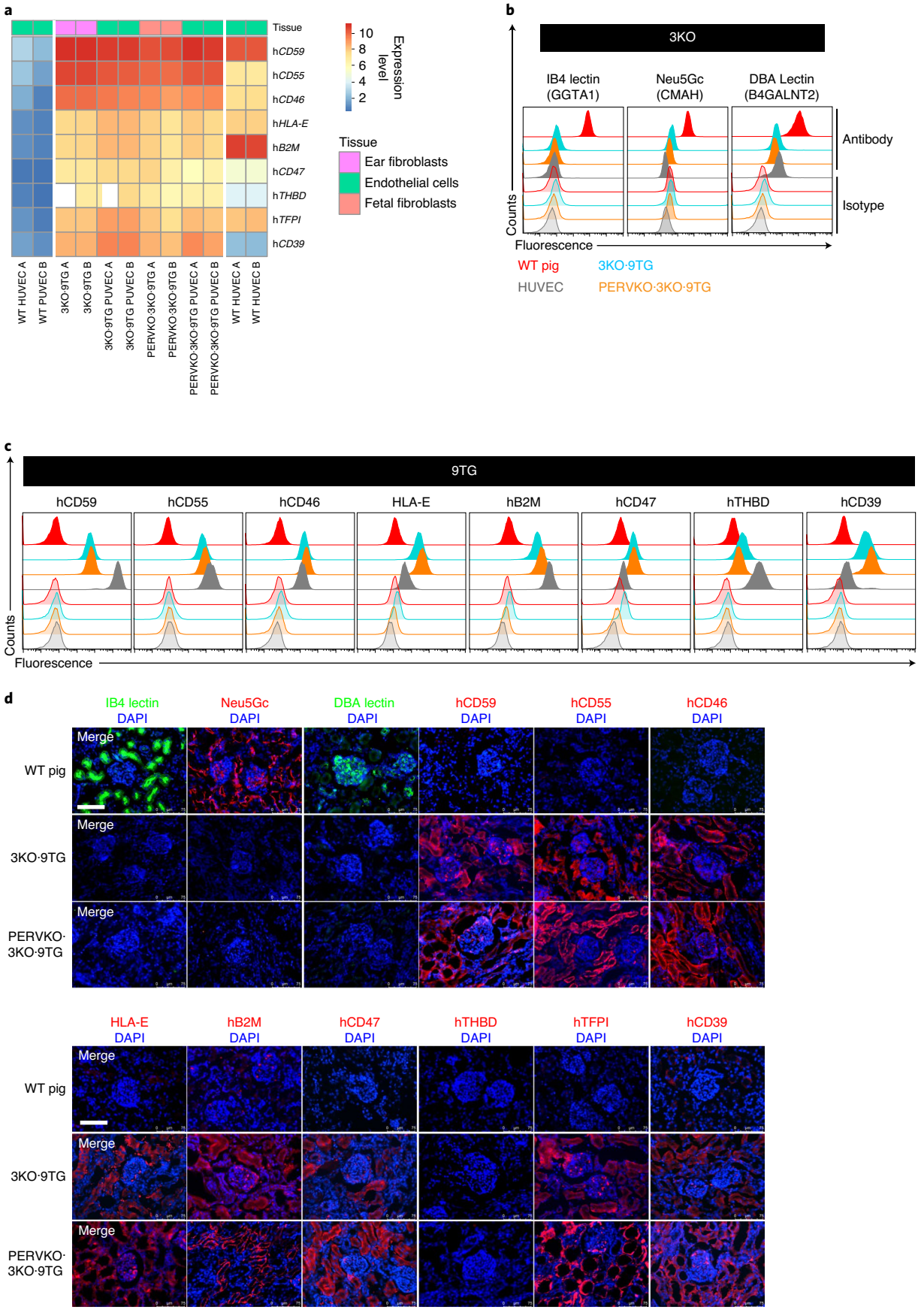

advanced genome engineering tools and created PERVKO·3KO·9TG pigs in which 13 genes and 42 alleles were modified. These genes were modified to eliminate PERV activity and to enhance human immunological and coagulation compatibility. Extensive analysis showed that our engineered pig cells showed reduced human antibody binding, complement toxicity, NK cell toxicity and coagulation dysregulation. Furthermore, our genome-modified pigs demonstrated normal pathophysiology, fertility and genetic inheritability. The successful production of PERVKO·3KO·9TG pigs has taken us a step forwards in clinical xenotransplantation.

The creation of PERVKO·3KO·9TG pigs demonstrates the power of synthetic biology to transform mammalian germlines extensively. Previous studies have used gene-stacking technology to insert multiple genes into the pig genome[35], a task that requires multiple rounds of genome editing and pig production. Alternatively, successful insertion of five transgenes into the pig genome has been reported[35] by co-delivering multiple separate transgene plasmids; however, the location, gene copy number, inheritability and expression level of these transgenes remains to be elucidated. In PERVKO·3KO·9TG pigs, we deleted the 25 copies of PERV elements found in the porcine genome and 8 alleles of the genes encoding 3 prominent targets of xeno-antibody, while concurrently expressing 9 human transgenes. This was all carried out using only two rounds of gene editing and cloning. Furthermore, we demonstrated the successful expression and function of these intended genetic modifications and validated its genetic inheritability.

The degree of genome modification needed to ensure safe and effective xenotransplantation remains to be determined. Since the early 2000s, the genetic manipulation of GTKO and human CRP transgenes (h*CD46* and h*CD55*) were among the earliest targets for engineered pigs and had been proven to be beneficial for xenotransplantation[36]. Recent advances in gene editing technology have enabled extensive genome editing in a high-throughput manner, leading to a growing list of available genetically modified pigs to enhance xenotransplantation compatibility. Nevertheless, although a few genetic modifications have improved xenograft survival in preclinical heart and kidney xenotransplantation studies[37,38], these survival outcomes need to be further studied in expanded trials before such preclinical xenotransplantation studies can be translated into clinical practice[38]. Moreover, the NHP recipients in these preclinical models were highly immunosuppressed. Besides the conventional immunosuppressant regimen, many costimulatory blockers and anti-inflammatory drugs were used off-label to support the long-term survival of the xenograft[37,38]

We believe that PERVKO·3KO·9TG pigs provide an alternative route to translate xenotransplantation into clinical practice by enhancing human immune tolerance to pig organs. Our genetic modifications in engineered pigs mainly aim to (1) reduce HAR caused by pre-formed antibodies and complement and (2) control innate cellular immunity of NK cells and macrophages—we believe that both of which are essential for the survival of the xenograft early on. Furthermore, (3) the humanization of some key coagulation regulatory factors in our pigs can help to mitigate xeno-specific coagulopathy[25,28], which cannot otherwise be addressed by immunosuppressants. Our in vitro assays clearly demonstrate the benefit of each category of modifications. Work is in progress to test the safety and effectiveness of PERVKO·3KO·9TG pig organs in NHP models.

We have also identified some opportunities for improvement in the future. For example, compared with the other transgene products, we did not detect THBD using either immunofluorescence or western blot, despite having detectable RNA-level expression. We are investigating several mechanisms that may explain this, including transgene isoform selection, post-transcriptional and post-translational modifications, and cellular localization in porcine hosts. Recent studies have also shown that the deletion of porcine major histocompatibility complex class I (MHC-I), also known as swine leucocyte class I (SLA-I), can reduce human antibody binding to porcine blood cells; this suggests that SLA-I may be another potential target for genetic modification[44]. For liver xenotransplantation, it may be potentially beneficial to knock out *ASGR1* (encoding asialoglycoprotein receptor 1) and/or *VWF* (encoding von Willebrand factor) to protect the xenograft from non-specific human platelet consumption[36,45].

Taken together, we believe that extensive genetic engineering holds great potential to translate xenotransplantation into a clinical promise. Furthermore, with the ability to execute complex genetic germline engineering, we are in a position to engineer additional functions in large animals. We envision that PERVKO·3KO·9TG pigs can be further genetically engineered to achieve additional

Fig. 4 | Functional validation of PERVKO·3KO·9TG pigs in mitigating human antibody binding, complement toxicity and NK cell toxicity, and modulating coagulation function. a–c, Compared with WT PUVECs, 3KO·9TG PUVECs and PERVKO·3KO·9TG PUVECs show significantly reduced binding to human IgG (**a**) and IgM (**b**). Antibody binding of pooled human serum to PUVECs and HUVECs (positive control) was measured using FACS. $n=3$ biologically independent samples. EC, endothelial cells. MFI, mean fluoresence intensity. For **a**, **b** and **d**–**g**, data are mean ± s.d. *P* values were determined using unpaired two-tailed Student's *t*-tests; $^{***}P<0.001$, $^{**}P<0.01$, $^{*}P<0.05$; NS, not significant ($P>0.05$). For **a**, $P=0.0039$ (3KO·9TG versus WT PUVEC), $P=0.0041$ (PERVKO·3KO·9TG versus WT PUVEC) and $P=0.0645$ (3KO·9TG versus PERVKO·3KO·9TG). For **b**, $P=0.0056$ (3KO·9TG versus WT PUVEC), $P=0.0059$ (PERVKO·3KO·9TG versus WT PUVEC) and $P=0.5388$ (3KO·9TG versus PERVKO·3KO·9TG). **d**, 3KO·9TG PUVECs and PERVKO·3KO·9TG PUVECs show comparable antibody-dependent complement cytotoxicity to HUVECs and significantly lower antibody-dependent complement cytotoxicity compared with WT PUVECs. $n=4$ biologically independent samples. Statistical analysis was performed using unpaired two-tailed Student's *t*-tests. $P=0.0116$ (3KO·9TG versus WT PUVEC at 25% HC (human complement (HC) diluted to 25% by Prigrow II serum-free basic medium)), $P=0.0120$ (PERVKO·3KO·9TG versus WT PUVEC at 25% HC), $P=0.0132$ (HUVEC versus WT PUVEC at 25% HC), $P=0.0109$ (3KO·9TG versus WT PUVEC at 50% HC), $P=0.0108$ (PERVKO·3KO·9TG versus WT PUVEC at 50% HC), $P=0.0112$ (HUVEC versus WT PUVEC at 50% HC), $P=0.0005$ (3KO·9TG versus WT PUVEC at 75% HC), $P=0.0012$ (PERVKO·3KO·9TG versus WT PUVEC at 75% HC) and $P=0.0026$ (HUVEC versus WT PUVEC at 75% HC). **e**, 3KO·9TG PUVECs and PERVKO·3KO·9TG PUVECs show significantly lower NK-cell-mediated cytotoxicity compared with their WT counterpart. $n=6$ biologically independent samples. Statistical analysis was performed using unpaired two-tailed Student's *t*-tests. $P=0.0070$ (3KO·9TG versus WT PUVEC), $P=0.0028$ (PERVKO·3KO·9TG versus WT PUVEC) and $P=0.0132$ (HUVEC versus WT PUVEC). **f**, Compared with WT PUVECs, 3KO·9TG PUVECs and PERVKO·3KO·9TG PUVECs reveal reduced phagocytosis by a human macrophage cell line. $n=4$ biologically independent samples. Statistical analysis was performed using unpaired, two-tailed Student's *t*-tests. $P=0.0161$ (3KO·9TG versus WT PUVEC), $P=0.0177$ (PERVKO·3KO·9TG versus WT PUVEC) and $P=0.0168$ (HUVEC versus WT PUVEC). **g**, 3KO·9TG PUVECs and PERVKO·3KO·9TG PUVECs mediate a very low level of TAT formation after incubation with whole human blood for the indicated time, which is comparable to HUVECs and significantly lower than WT PUVECs. $n=4$ biologically independent samples. Statistical analysis was performed using unpaired two-tailed Student's *t*-tests. $P=0.0026$ (3KO·9TG versus WT PUVEC at 15 min), $P=0.0031$ (PERVKO·3KO·9TG versus WT PUVEC at 15 min), $P=0.0030$ (HUVEC versus WT PUVEC at 15 min), $P=0.0019$ (3KO·9TG versus WT PUVEC at 45 min), $P=0.0019$ (PERVKO·3KO·9TG versus WT PUVEC at 45 min), $P=0.0018$ (HUVEC versus WT PUVEC at 45 min); $^{***}P<0.001$. The gating strategies for **a**–**f** are shown in Supplementary Fig. 16.

functions, such as immune tolerance[46], organ longevity[47] and viral immunity[48–50].

Methods

CRISPR–Cas9 gRNA design. We used the R library DECIPHER to design specific gRNAs (PERV-3N, 5′-TCTGGCGGGAGCCACCAAAC-3′; PERV-5N, 5′-GGCTTCGTCAAAGATGGTCG-3′; PERV-9N, 5′-TTCTAAGCAGTCCTGTTTGG-3′) to specifically target all *pol* catalytic sequences in the 3KO·9TG genome as described previously[6]. Furthermore, we used specific gRNAs to target *GGTA1*, *CMAH* and *B4GALNT2*, respectively (*GGTA1*, 5′-GCTGCTTGTCTCAACTGTAA-3′; *CMAH*, 5′-GAAGCTGCCAATCTCAAGGA-3′; *B4GALTN2*, 5′- GATGCCCGAAGGCGTCACAT-3′).

Cell culture. Porcine fetal fibroblast cells and ear fibroblast cells were maintained in Dulbecco's modified Eagle's medium (DMEM, Invitrogen) high glucose with sodium pyruvate supplemented with 20% fetal bovine serum (Invitrogen), 100 U ml^{-1} penicillin–streptomycin (Invitrogen) and 10 mM HEPES (Thermo Fisher Scientific). All cells were maintained in a humidified tri-gas incubator at 37 °C under 5% CO_2, 90% N_2 and 5% O_2. PUVECs were freshly isolated and cultured in Prigrow II medium (abm) supplemented with 10% fetal bovine serum (Gibco), 100 U ml^{-1} penicillin–streptomycin (Invitrogen) and 10 mM HEPES (Thermo Fisher Scientific). HUVECs (ATCC, PCS-100-010) were cultured in vascular cell basal medium supplemented with the Endothelial Cell Growth Kit-BBE (ECG kit, ATCC). The human NK-92 cell line was cultured in MEM α (Gibco) supplemented with 12.5% fetal bovine serum (Gibco), 12.5% fetal equine serum (FES, Solarbio) and 100 U ml^{-1} penicillin–streptomycin (Invitrogen). The human macrophage cell line THP-1 was cultured in RPMI 1640 (BI) supplemented

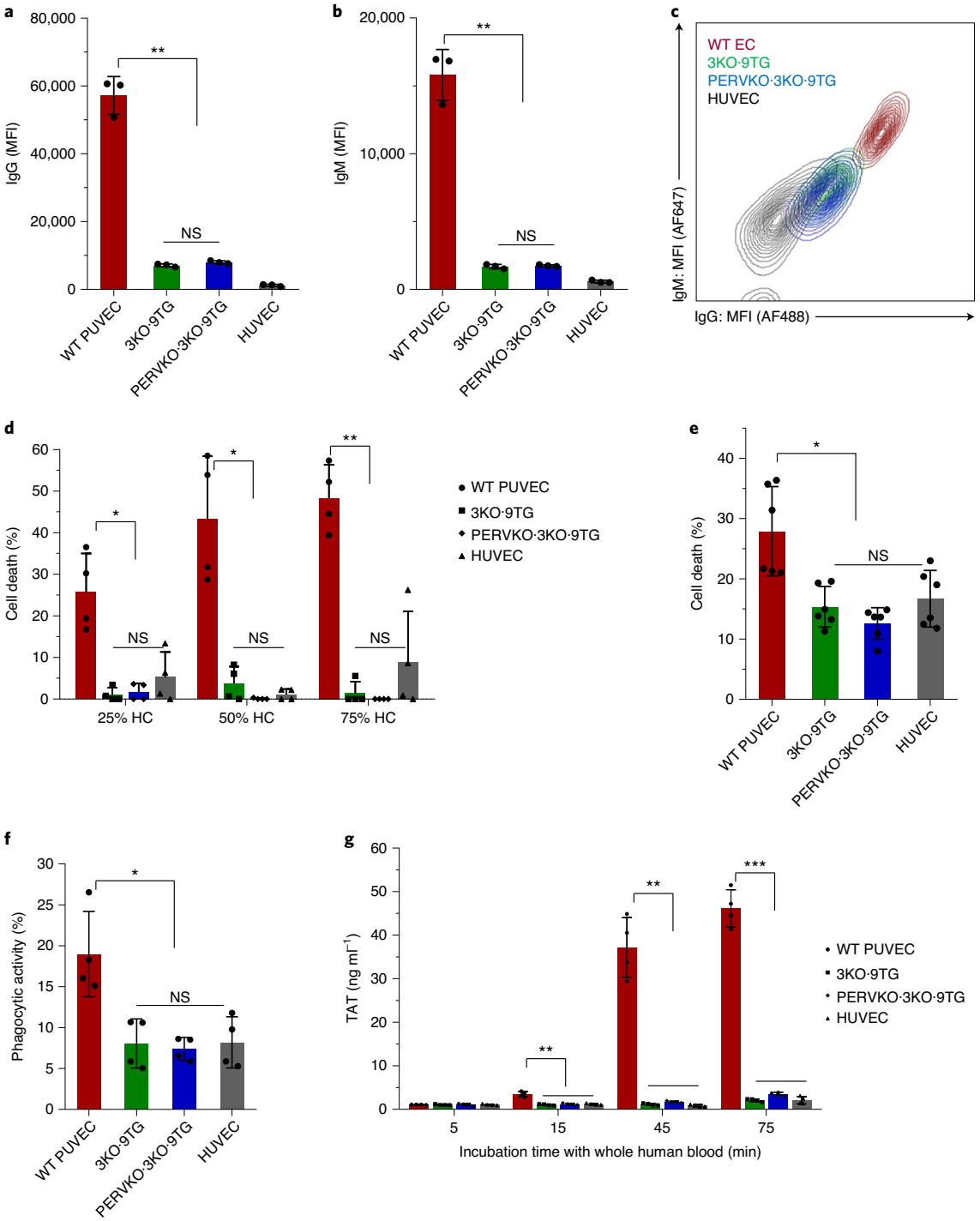

with 10% fetal bovine serum (Gibco) and 100 U ml^{-1} penicillin–streptomycin (Invitrogen). Differentiation of THP-1 cells was achieved in 62.5 nM phorbol-12-myristate-13-acetate (PMA, Sigma-Aldrich) for 3 d and confirmed by attachment of these cells to the tissue-culture plastic.

3KO·9TG cell production. To generate 3KO·9TG cells (where 3KO denotes the triple knockout of the porcine *GGTA1*, *CMAH* and *B4GALNT2* genes, while 9TG denotes the expression of nine human transgenes, including h*CD46*, h*CD55*, h*CD59*, h*THBD*, h*TFPI*, h*CD39*, h*B2M*, *HLA-E* and h*CD47*), we transfected 1 million porcine ear fibroblasts with 2.5 μg *Cas9* expression plasmid, 1.5 μg *B4GALNT2*, 1.0 μg *CMAH* and 0.5 μg *GGTA* gRNA expression plasmids, 1 μg Super PiggyBac plasmid (PB210PA-1, System Biosciences) and 4 μg transgene expression plasmid. Then, 9 d after transfection, cells were stained with antibodies against isolectin B4 (GGTA1, ALX-650-001F-MC05, Enzo), CD46 (A15776, Invitrogen) and CD39 (560239, BD Biosciences). Subsequently, cells that were negative for GGTA1 and positive for both CD46 and CD39 were sorted into 96-well plates using a SONY SH800S cell sorter. When individual clones reached 30–50% confluency, cells were transferred and expanded, whereas aliquots were used to genotype using the KAPA mouse genotyping kit (KR0385, KAPA Biosystems). The 3KO was genotyped using NGS, and the presence of 9TG was confirmed by PCR using the primers listed in Supplementary Table 1.

PERVKO·3KO·9TG cell production. The 3KO·9TG ear fibroblasts were edited to generate PERVKO·3KO·9TG as previously described[6]. We also genotyped the clones derived from the sorted single cells. The procedure for genotyping was described previously[51]. In brief, we sorted single cells into 96-well PCR plates with each well carrying a 5 μl lysis mixture, which contained 0.5 μl 10× KAPA express extract buffer (KAPA Biosystems), 0.1 μl of 1 U μl^{-1} KAPA Express Extract Enzyme and 4.4 μl water. We incubated the lysis reaction at 75 °C for 15 min and inactivated the reaction at 95 °C for 5 min. All reactions were then added to 20 μl PCR reactions containing 1× KAPA 2G fast (KAPA Biosystems) and 0.2 μM PERV Illumina primers as follows: Illumina_PERV_pol forward, 5′-ACACTCTTTCCCTACACGACG CTCTTCCGATCTCGACT GCCCCAAGGGTTCAA-3′; Illumina_PERV_pol reverse, 5′-GTGACTGGAGTT CAGACGTGTGCTCTTCCGATC TTCTCTCCTGCAAATCTGGGCC-3′.

Reactions were incubated at 95 °C for 3 min followed by 30 (for single cell) or 25 (for single-cell clones) cycles of 95 °C for 20 s, 59 °C for 20 s and 72 °C for 10 s. To add the Illumina sequence adaptors, 3 μl of reaction products was then added to 20 μl of PCR mix containing 1× KAPA 2G fast (KAPA Biosystems) and 0.3 μM primers carrying Illumina sequence adaptors. Reactions were incubated at 95 °C for 3 min, followed by 20 (for single cell) or 10 (for single-cell clones) cycles of 95 °C for 20 s, 59 °C for 20 s and 72 °C for 10 s. PCR products were examined on 3% agarose gels. These products were then mixed at roughly the same quantity, purified using the SPRIselect Reagent Kit (Beckman Coulter, B23317) or AMPure XP Beads (Beckman Coulter, A63881), and sequenced using a HiSeq X or NovaSeq (Illumina) system. We then analysed deep-sequencing data to determine the PERV editing efficiency.

Somatic cell microinjection to produce SCNT embryos and embryo transfer for pig cloning. The somatic cell microinjection procedure was reported previously[52]. All of the animal experiments were approved by the Animal Care Committee of Yunnan Agricultural University, China. All of the chemicals were purchased from Sigma Chemical unless otherwise indicated. Porcine ovaries were collected from Hongteng Abattoir (Chenggong Ruide Food). The ovaries were transported to the laboratory at 25–30 °C in 0.9% (w/v) NaCl solution supplemented with 75 mg ml^{-1} potassium penicillin G and 50 mg ml^{-1} streptomycin sulfate. The cumulus cell–oocyte complexes (COCs) were isolated from the follicles of 3–6 mm in diameter, and then cultured in 200 μl TCM-199 medium supplemented with 0.1 mg ml^{-1} pyruvic acid, 0.1 mg ml^{-1} L-cysteine hydrochloride monohydrate, 10 ng ml^{-1} epidermal growth factor, 10% (v/v) porcine follicular fluid, 75 mg ml^{-1} potassium penicillin G, 50 mg ml^{-1} streptomycin sulfate, and 10 IU ml^{-1} eCG and hCG (Teikoku Zouki) at 38.5 °C in a humidified atmosphere with 5% CO_2 (APC-30D, ASTEC). After 38–42 h in vitro maturation, the expanded cumulus cells of the COCs were removed by repeat pipetting of the COCs in 0.1% (w/v) hyaluronidase.

SCNT was conducted as previously described[53,54]. In brief, oocytes extruding the first polar body with an intact membrane were cultured in NCSU23 medium supplemented with 0.1 mg ml^{-1} demecolcine, 0.05 M sucrose and 4 mg ml^{-1} bovine serum albumin (BSA) for 0.5–1 h for nucleus protrusion. The protruded nucleus was then removed along with the polar body using a bevelled pipette (approximately 20 μm in diameter) in Tyrode's lactate medium supplemented with 10 μM HEPES, 0.3% (w/v) polyvinylpyrrolidone and 10% FBS in the presence of 0.1 mg ml^{-1} demecolcine and 5 mg ml^{-1} cytochalasin B. Fibroblasts with confirmed genotypes were used as nuclear donors. A single donor cell was injected into the perivitelline space of the enucleated oocyte.

Donor cells were fused with the recipient cytoplasts with a single direct current pulse of 200 V mm^{-1} for 20 μs using an embryonic cell fusion system (ET3, Fujihira Industry) in a fusion medium containing 0.25 M D-sorbic alcohol, 0.05 mM $Mg(C_2H_3O_2)_2$, 20 mg ml^{-1} BSA and 0.5 mM HEPES (free acid). The reconstructed embryos were cultured in PZM-3 solution[54] for 2 h to allow nucleus reprogramming and were then activated with a single pulse of 150 V mm^{-1} for 100 μs in an activation medium containing 0.25 M D-sorbic alcohol, 0.01 mM $Ca(C_2H_3O_2)_2$, 0.05 mM $Mg(C_2H_3O_2)_2$ and 0.1 mg ml^{-1} BSA. The activated embryos were then cultured in PZM-3 supplemented with 5 mg ml^{-1} cytochalasin B for 2 h at 38.5 °C in humidified atmosphere with 5% CO_2, 5% O_2 and 90% N_2 (APM-30D for further activation, ASTEC). Reconstructed embryos were then transferred to new PZM-3 medium and cultured in humidified air with 5% CO_2, 5% O_2 and 90% N_2 at 38.5 °C for 2 d and 7 d to detect the embryo cleavage and blastocyst development ratios, respectively.

Crossbred (Large White/Landrace Duroc) sows with one birth history were used as the surrogate mothers of the constructed embryos. They were examined for oestrus at 09:00 and 18:00 daily. The SCNT embryos cultured for 6 h after activation were surgically transferred to the oviducts of the surrogates. Pregnancy was examined 23 d after embryo transfer using an ultrasound scanner (HS-101 V, Honda Electronics).

Validation of genetic modification at the protein level using FACS. Umbilical vein endothelial cells derived from 3KO·9TG, PERVKO·3KO·9TG and WT pigs were analysed using FACS to characterize the genetic modifications (3KO and 9TG) at the protein level. Cells were collected, fixed and then stained using the corresponding primary and secondary antibodies (Supplementary Table 2), according to manufacturer's instructions. Isotype controls were applied at the same final dilution as the specific primary antibodies. After antibody staining, cells were washed twice and analysed by FACS using a CytoFLEX S flow cytometer. We analysed 5,000 events for each sample using the Flow Jo software.

Characterization of protein expression by immunofluorescence. Neonatal (aged 3–6 d) porcine kidney and heart cryosections of WT, 3KO·9TG and PERVKO·3KO·9TG pigs were analysed using immunofluorescence to characterize the genetic modification (3KO and 9TG) at the tissue level. Cryosections were fixed with ice-cold acetone, blocked and then stained using either one-step direct or two-step indirect immunofluorescence techniques. A summary of the primary and secondary antibodies used is provided in Supplementary Table 2. Nuclear staining was performed using ProLong Gold DAPI (Thermo Fisher Scientific, P36931). Sections were imaged using a Leica fluorescence microscope and analysed using ImageJ. All of the pictures were taken under the same conditions to enable accurate comparison of fluorescence intensities among WT, 3KO·9TG and PERVKO·3KO·9TG cryosections.

Western blotting. Cells and tissues were lysed in RIPA buffer (Thermo Fisher Scientific, 89900) supplemented with the Halt protease inhibitor cocktail (Thermo Fisher Scientific, 78430). Tissues were homogenized (Shanghai Jing Xin, Tiss-24) and sonicated (QSONICA, Q125). Protein concentration was determined using the Pierce BCA Protein Assay Kit (Thermo Fisher Scientific, 23225). Western blotting was performed by conventional techniques using 10% and 15% SDS–PAGE gels (EpiZyme, PG113) and polyvinylidene difluoride membrane (Millipore, ISEQ00010). Blots were blocked in Tris-buffered saline with 0.1% (v/v) Tween-20 (TBST) blocking buffer containing 5% milk for 1 h at room temperature and then incubated overnight with primary antibodies diluted in Universal Antibody Diluent (NCM, WB500D) at 4°C. Subsequently, blots were washed and incubated with appropriate HRP labelled secondary antibodies in TBST for 1 h at room temperature. A summary of the primary and secondary antibodies used is provided in Supplementary Table 2. The blots were then incubated with ECL Western Blotting Substrate (Tanon, 180–501) and luminescence was captured by using a Bio-Rad ChemiDoc XRS.

Human antibody binding to porcine endothelial cells. Binding of human IgG and IgM to the porcine and human endothelial cells was assessed using flow cytometry as described previously[55]. In brief, PUVECs and HUVECs were collected, washed twice and resuspended in staining buffer (PBS containing 1% BSA). Heat-inactivated pooled normal human male AB serum (Innovative Research) was diluted 1:4 in staining buffer. 3KO·9TG PUVECs, PERVKO·3KO·9TG PUVECs, WT PUVECs and HUVECs (1×10^5 cells per test) were incubated with diluted human serum for 30 min at room temperature, respectively. Cells were then washed with cold staining buffer and incubated with goat anti-human IgG Alexa Fluor 488 (Invitrogen, A11013, 1:200 dilution) and goat anti-human IgM Alexa Fluor 647 (Invitrogen, A21249, 1:200 dilution) for 30 min at room temperature. After washing with cold staining buffer, cells were resuspended in staining buffer containing 7-AAD (559925, BD Biosciences; 1:100 dilution) to exclude non-viable cells. Fluorescence was acquired using a CytoFLEX S flow cytometer and data were analysed using FlowJo analysis software as previously described[55].

Human complement-dependent cytotoxicity assay. 3KO·9TG PUVECs, PERVKO·3KO·9TG PUVECs, WT PUVECs and HUVECs were collected, washed twice with PBS and resuspended in serum-free culture medium. Cells (1×10^5 cells per test) were incubated with a uniform pool of human serum complement (A113, Quidel) at different concentrations (0%, 25%, 50% and 75%) for 45 min at 37 °C and 5% CO_2. Cells were then stained with propidium iodide (PI; P3566, Invitrogen; 1:500 dilution) for 5 min and analysed using a CytoFLEX S flow cytometer. The percentage of PI-positive cells was used as the percentage of cell death.

NK cell cytotoxicity assay. PUVECs and HUVECs were used as target cells and labelled with anti-pig CD31-FITC (Bio-Rad, MCA1746F) and anti-human CD31-FITC (BD, 555445) antibodies, respectively. Meanwhile, human NK-92 cells were used as effector cells and labelled with anti-human CD56-APC antibodies (BD, 555518). The effector (E) and target cells (T) were cocultured for 4 h at 37 °C and 5% CO_2, at an E:T ratio of 3:1. Cells were stained with propidium iodide for 5 min and then analysed using FACS. The percentage of PI-positive cells in the $CD31^+$ gate was used to calculate the percentage of killed target cells.

Phagocytosis assay. Differentiation of human macrophage cell line THP-1 was achieved by 62.5 nM of PMA for 3 d and confirmed by attachment of these cells to tissue culture plastic. 3KO·9TG PUVECs, PERVKO·3KO·9TG PUVECs, WT PUVECs and HUVECs (target cells) were stained with the fluorescent dyes 5/6-CFSE (Molecular Probes) according to the manufacturer's protocol. CFSE-labelled target cells were incubated with human differentiated THP-1 cells (effector cells) at an E:T ratio of 1:2 for 4 h at 37 °C. Macrophages were counterstained with anti-human CD11b antibodies (Thermo Fisher Scientific, 17-0112-81) and phagocytosis of CFSE-labelled targets was measured using FACS. Phagocytic activity was calculated as previously described[21].

CD39 biochemical ADPase assay. 3KO·9TG PUVECs, PERVKO·3KO·9TG PUVECs, WT PUVECs and HUVECs were seeded at 2×10^4 per well in a 96-well plate 1 d before the assay. Cells were incubated with 500 μM ADP (Chrono-Log, 384) for 30 min at 37 °C and 5% CO_2. Malachite green (MAK307, Sigma-Aldrich) was added to stop the reaction, and absorbance was measured at 630 nm to determine the levels of phosphate generation against the standard curve of KH_2PO_4.

TFPI activity and human-factor-Xa-binding assay. To prepare for the assay, cells were treated with 1 μM PMA for 6 h to promote hTFPI translocation to the cell surface of 3KO·9TG and PERVKO·3KO·9TG PUVECs. TFPI activity and human-factor-Xa-binding assay was subsequently performed as previously described previously[55]. All assays were performed in quadruplicate.

TAT formation assay. 3KO·9TG PUVECs, PERVKO·3KO·9TG PUVECs, WT PUVECs and HUVECs were seeded at 3×10^5 per well in six-well plates. After 1 d, cells were incubated with 1 ml of fresh whole human blood (containing 0.5 U ml^{-1} heparin) at 37 °C with gentle shaking. At the different indicated time points, blood was aspirated, from which plasma was isolated. TAT content in the plasma was measured using a Human Thrombin–Antithrombin Complex ELISA Kit (ab108907, Abcam).

Variant calling from whole genome sequencing data. Paired reads were mapped to the *Sus scrofa* 11.1 genome (ftp://ftp.ensembl.org/pub/release-91/fasta/sus_scrofa/dna/) using BWA (v.0.7.17-r1188)[56]. Variants (SNPs and INDELs) were called using GATK (v.4.0.7.0)[57] according to the GATK best practice recommendation[58] with the standard filter plus requiring a minimum depth of 10.

In silico prediction of on/off-target sites. Genome-wide on-target and off-target sites were predicted using CRISPRSeek (v.1.22.1)[59] in R (v.3.5.0), allowing for up to four mismatches. The input genome was *Sus scrofa* 11.1 (ftp://ftp.ensembl.org/pub/release-91/fasta/sus_scrofa/dna/).

Off-target calling from WGS data. Variants from GATK within a 10 bp distance of the protospacer adjacent motif sites of CRISPRSeek (v.1.22.1)[59]-predicted off-targets were called as potential off-target modifications. Variants with an allele frequency deviating significantly by ±0.5 from the parental line were filtered out using two-proportion *Z*-tests. The assumption for this test is that the probability that both alleles are simultaneously modified is very low because the introduction of off-target mutations by CRISPR–Cas9 genome editing is very rare[41].

Functional impact analysis of variants. Regardless of whether a variant was an off-target or germline mutation, it was annotated for sequence change at the transcript level and amino acid change at the protein level to assess its potential functional impact using VEP (variant effect predictor, v.93.3)[60]. High impact variants were selected if they could result in frameshift, start gain/lost, stop gain/lost, splice donor/acceptor shift or splice region changes. Whenever available, the variant was annotated to indicate whether it impacts principle or alternative transcripts using the APPRIS database[61].

Transcription analysis using RNA-seq. RNA-seq reads were aligned to the *Sus Scrofa* 11.1 genome using STAR (v.2.6.1a)[62] under the splicing-aware mode. The expression level was quantified as transcripts per million using Salmon (v.0.11.3)[63], with both the porcine transcriptome and the nine transgenes as reference transcripts.

PERV knock-out efficiency analysis using deep sequencing. Paired reads were first aligned to the PERV capture target sequence using STAR (v.2.6.1a)[62] under the splicing-aware mode, followed by alignment position dependent deduplication using Picard (v.2.18.14). Deduped paired reads were then merged into fragments. Merged fragments were realigned to the PERV capture target sequence using STAR (v.2.6.1a)[62] under the splicing-aware mode. Each CIGAR flag of the realigned BAM file was then analysed to determine whether the INDELs within the target region collectively confer a frameshift knock-out. Finally, the PERV knock-out efficiency was calculated as the percentage of molecular fragments that have a frameshift knock-out.

Statistical analysis. All statistical analyses were performed using R (v.3.5.0) and Excel (v.2016). $P<0.05$ was considered to be significant unless otherwise specified. When multiple tests were involved simultaneously, *P*-value correction was performed using the Benjamini–Hochberg procedure to control for the overall false-discovery rate. A false-discovery-rate-corrected $P<0.05$ was typically used unless otherwise specified.

Reporting Summary. Further information on research design is available in the Nature Research Reporting Summary linked to this article.

Data availability

The main data supporting the findings of this study are available within the paper and its Supplementary Information. Data from the RNA-seq analyses are available at figshare (https://doi.org/10.6084/m9.figshare.12841418.v1). The raw data generated during the study are available at the China National GeneBank, with the accession code CNP0001254. The pig reference genome (*Sus scrofa* 11.1) sequence was obtained from Ensembl (ftp://ftp.ensembl.org/pub/release-91/fasta/sus_scrofa/dna). The pig transcript isoform information was obtained from the APPRIS database (http://appris.bioinfo.cnio.es/#/seeker).

Received: 29 January 2020; Accepted: 22 August 2020;
Published online: 21 September 2020

References

1. Sykes, M. & Sachs, D. H. Transplanting organs from pigs to humans. *Sci. Immunol.* **4**, eaau6298 (2019).
2. Cooper, D. K. C., Ekser, B. & Tector, A. J. Immunobiological barriers to xenotransplantation. *Int. J. Surg.* **23**, 211–216 (2015).
3. Denner, J. & Tonjes, R. R. Infection barriers to successful xenotransplantation focusing on porcine endogenous retroviruses. *Clin. Microbiol Rev.* **25**, 318–343 (2012).
4. Patience, C., Takeuchi, Y. & Weiss, R. A. Infection of human cells by an endogenous retrovirus of pigs. *Nat. Med.* **3**, 282–286 (1997).
5. Shin, J. S. et al. Minimizing immunosuppression in islet xenotransplantation. *Immunotherapy* **6**, 419–430 (2014).
6. Niu, D. et al. Inactivation of porcine endogenous retrovirus in pigs using CRISPR-Cas9. *Science* **357**, 1303–1307 (2017).
7. Cooper, D. K. Modifying the sugar icing on the transplantation cake. *Glycobiology* **26**, 571–581 (2016).
8. Byrne, G., Ahmad-Villiers, S., Du, Z. & McGregor, C. B4GALNT2 and xenotransplantation: a newly appreciated xenogeneic antigen. *Xenotransplantation* **25**, e12394 (2018).
9. Song, K. H. et al. Cloning and functional characterization of pig CMP-*N*-acetylneuraminic acid hydroxylase for the synthesis of *N*-glycolylneuraminic acid as the xenoantigenic determinant in pig-human xenotransplantation. *Biochem. J.* **427**, 179–188 (2010).
10. Estrada, J. L. et al. Evaluation of human and non-human primate antibody binding to pig cells lacking GGTA1/CMAH/beta4GalNT2 genes. *Xenotransplantation* **22**, 194–202 (2015).
11. Phelps, C. J. et al. Production of α1,3-galactosyltransferase-deficient pigs. *Science* **299**, 411–414 (2003).
12. Lai, L. et al. Production of α-1,3-galactosyltransferase knockout pigs by nuclear transfer cloning. *Science* **295**, 1089–1092 (2002).
13. Martens, G. R. et al. Humoral reactivity of renal transplant-waitlisted patients to cells from GGTA1/CMAH/B4GalNT2, and SLA class I knockout pigs. *Transplantation* **101**, e86–e92 (2017).
14. Yamada, K. et al. Marked prolongation of porcine renal xenograft survival in baboons through the use of α1,3-galactosyltransferase gene-knockout donors and the cotransplantation of vascularized thymic tissue. *Nat. Med.* **11**, 32–34 (2005).
15. Kuwaki, K. et al. Heart transplantation in baboons using α1,3-galactosyltransferase gene-knockout pigs as donors: initial experience. *Nat. Med.* **11**, 29–31 (2005).
16. Cooper, D. K., Ekser, B., Ramsoondar, J., Phelps, C. & Ayares, D. The role of genetically engineered pigs in xenotransplantation research. *J. Pathol.* **238**, 288–299 (2016).
17. Mohiuddin, M. M. et al. B-cell depletion extends the survival of GTKO. hCD46*Tg* pig heart xenografts in baboons for up to 8 months. *Am. J. Transpl.* **12**, 763–771 (2012).

18. Zhou, C. Y. et al. Transgenic pigs expressing human CD59, in combination with human membrane cofactor protein and human decay-accelerating factor. *Xenotransplantation* **12**, 142–148 (2005).
19. Griesemer, A., Yamada, K. & Sykes, M. Xenotransplantation: immunological hurdles and progress toward tolerance. *Immunol. Rev.* **258**, 241–258 (2014).
20. Lilienfeld, B. G., Crew, M. D., Forte, P., Baumann, B. C. & Seebach, J. D. Transgenic expression of HLA-E single chain trimer protects porcine endothelial cells against human natural killer cell-mediated cytotoxicity. *Xenotransplantation* **14**, 126–134 (2007).
21. Ide, K. et al. Role for CD47-SIRPα signaling in xenograft rejection by macrophages. *Proc. Natl Acad. Sci. USA* **104**, 5062–5066 (2007).
22. Siegel, J. B. et al. Xenogeneic endothelial cells activate human prothrombin. *Transplantation* **64**, 888–896 (1997).
23. Lee, K. F. et al. Recombinant pig TFPI efficiently regulates human tissue factor pathways. *Xenotransplantation* **15**, 191–197 (2008).
24. Choi, C. Y. et al. Pig tissue factor pathway inhibitor α fusion immunoglobulin inhibits pig tissue factor activity in human plasma moderately more efficiently than the human counterpart. *Biotechnol. Lett.* **39**, 1631–1638 (2017).
25. Robson, S. C., Cooper, D. K. & d'Apice, A. J. Disordered regulation of coagulation and platelet activation in xenotransplantation. *Xenotransplantation* **7**, 166–176 (2000).
26. Ji, H. et al. Pig BMSCs transfected with human TFPI combat species incompatibility and regulate the human TF pathway in vitro and in a rodent model. *Cell. Physiol. Biochem.* **36**, 233–249 (2015).
27. Kopp, C. W. et al. Effect of porcine endothelial tissue factor pathway inhibitor on human coagulation factors. *Transplantation* **63**, 749–758 (1997).
28. Iwase, H., Ezzelarab, M. B., Ekser, B. & Cooper, D. K. The role of platelets in coagulation dysfunction in xenotransplantation, and therapeutic options. *Xenotransplantation* **21**, 201–220 (2014).
29. Miwa, Y. et al. Potential value of human thrombomodulin and DAF expression for coagulation control in pig-to-human xenotransplantation. *Xenotransplantation* **17**, 26–37 (2010).
30. Mohiuddin, M. M. et al. Chimeric 2C10R4 anti-CD40 antibody therapy is critical for long-term survival of GTKO.hCD46.hTBM pig-to-primate cardiac xenograft. *Nat. Commun.* **7**, 11138 (2016).
31. Wheeler, D. G. et al. Transgenic swine: expression of human CD39 protects against myocardial injury. *J. Mol. Cell Cardiol.* **52**, 958–961 (2012).
32. Cooper, D. K. C. et al. Justification of specific genetic modifications in pigs for clinical organ xenotransplantation. *Xenotransplantation* **26**, e12516 (2019).
33. Samy, K. P., Martin, B. M., Turgeon, N. A. & Kirk, A. D. Islet cell xenotransplantation: a serious look toward the clinic. *Xenotransplantation* **21**, 221–229 (2014).
34. Matsumoto, S., Tomiya, M. & Sawamoto, O. Current status and future of clinical islet xenotransplantation. *J. Diabetes* **8**, 483–493 (2016).
35. Fischer, K. et al. Efficient production of multi-modified pigs for xenotransplantation by 'combineering', gene stacking and gene editing. *Sci. Rep.* **6**, 29081 (2016).
36. Yunga, G. L. P., Riebenb, R., Bühlerc, L., Schuurmanc, H. J. & Seebach, J. Xenotransplantation: where do we stand in 2016? *Swiss Med. Wkly* **147**, w14403 (2017).
37. Langin, M. et al. Consistent success in life-supporting porcine cardiac xenotransplantation. *Nature* **564**, 430–433 (2018).
38. Kim, S. C. et al. Long-term survival of pig-to-rhesus macaque renal xenografts is dependent on CD4 T cell depletion. *Am. J. Transpl.* **19**, 2174–2185 (2019).
39. Li, X. et al. PiggyBac transposase tools for genome engineering. *Proc. Natl Acad. Sci. USA* **110**, E2279–E2287 (2013).
40. Kim, S., Kim, D., Cho, S. W., Kim, J. & Kim, J. S. Highly efficient RNA-guided genome editing in human cells via delivery of purified Cas9 ribonucleoproteins. *Genome Res.* **24**, 1012–1019 (2014).
41. Zuo, E. et al. Cytosine base editor generates substantial off-target single-nucleotide variants in mouse embryos. *Science* **364**, 289–292 (2019).
42. Laird, C. T. et al. Transgenic expression of human leukocyte antigen-E attenuates GalKO.hCD46 porcine lung xenograft injury. *Xenotransplantation* **24**, e12294 (2017).
43. Chen, D. et al. Regulated inhibition of coagulation by porcine endothelial cells expressing P-selectin-tagged hirudin and tissue factor pathway inhibitor fusion proteins. *Transplantation* **68**, 832–839 (1999).
44. Fischer, K. et al. Viable pigs after simultaneous inactivation of porcine MHC class I and three xenoreactive antigen genes GGTA1, CMAH and B4GALNT2. *Xenotransplantation* **27**, e12560 (2020).
45. Ekser, B., Markmann, J. F. & Tector, A. J. Current status of pig liver xenotransplantation. *Int. J. Surg.* **23**, 240–246 (2015).
46. Zhao, Y. et al. Skin graft tolerance across a discordant xenogeneic barrier. *Nat. Med.* **2**, 1211–1216 (1996).
47. Jesus, B. B. D. et al. Telomerase gene therapy in adult and old mice delays aging and increases longevity without increasing cancer. *EMBO Mol. Med.* **4**, 691–704 (2012).
48. Kennedy, E. M. & Cullen, B. R. Gene editing: a new tool for viral disease. *Annu Rev. Med* **68**, 401–411 (2017).
49. Burkard, C. et al. Pigs lacking the scavenger receptor cysteine-rich domain 5 of CD163 are resistant to porcine reproductive and respiratory syndrome virus 1 infection. *J. Virol.* **92**, e00415-18 (2018).
50. Yan, Q. et al. Production of transgenic pigs over-expressing the antiviral gene Mx1. *Cell Regen.* **3**, 11 (2014).
51. Yang, L. et al. Genome-wide inactivation of porcine endogenous retroviruses (PERVs). *Science* **350**, 1101–1104 (2015).
52. Wei, H. et al. Comparison of the efficiency of banna miniature inbred pig somatic cell nuclear transfer among different donor cells. *PLoS ONE* **8**, e57728 (2013).
53. Tomii, R. et al. Production of cloned pigs by nuclear transfer of preadipocytes following cell cycle synchronization by differentiation induction. *J. Reprod. Dev.* **55**, 121–127 (2009).
54. Kurome, M. et al. Production efficiency and telomere length of the cloned pigs following serial somatic cell nuclear transfer. *J. Reprod. Dev.* **54**, 254–258 (2008).
55. Costa, C. & Manez, R. *Xenotransplantation: Methods and Protocols* 335 (Springer, xiHumana Press, 2012).
56. Li, H. & Durbin, R. Fast and accurate short read alignment with Burrows-Wheeler transform. *Bioinformatics* **25**, 1754–1760 (2009).
57. McKenna, A. et al. The genome analysis toolkit: a MapReduce framework for analyzing next-generation DNA sequencing data. *Genome Res.* **20** , 1297–1303 (2010).
58. DePristo, M. A. et al. A framework for variation discovery and genotyping using next-generation DNA sequencing data. *Nat. Genet.* **43**, 491–498 (2011).
59. Zhu, L. J., Holmes, B. R., Aronin, N. & Brodsky, M. H. CRISPRseek: a bioconductor package to identify target-specific guide RNAs for CRISPR-Cas9 genome-editing systems. *PLoS ONE* **9**, e108424 (2014).
60. McLaren, W. et al. The ensembl variant effect predictor. *Genome Biol.* **17**, 122 (2016).
61. Rodriguez, J. M. et al. APPRIS: annotation of principal and alternative splice isoforms. *Nucleic Acids Res.* **41**, D110–D117 (2013).
62. Dobin, A. et al. STAR: ultrafast universal RNA-seq aligner. *Bioinformatics* **29**, 15–21 (2013).
63. Patro, R., Duggal, G., Love, M. I., Irizarry, R. A. & Kingsford, C. Salmon provides fast and bias-aware quantification of transcript expression. *Nat. Methods* **14**, 417–419 (2017).

Acknowledgements

We thank G. Yang of Harvard University for reading our manuscript; Q. Tang and P. O'Connell for their advice; and Y. Yang and Q. Yang from Third Affiliated Hospital of Sun Yat-sen University, H. Liu from Henan Chuangyuan Biotechnology, and colleagues at Qihan Bio and eGenesis for their technical assistance and discussions. The pig cloning work was supported by National Key R&D Program of China (grant no. 2019YFA0110700).

Author contributions

L.Y., G.M.C. and Y.G. envisioned and supervised the whole project; H.-J.W. and H.-Y.Z. supervised pig cloning and production. Y.Y., W.X. and Y.K. designed the experiments and wrote the manuscript. Y.Y., Y.K., Y.Z., X.S., L.Lamriben, J.W., J.X., M.X., Q.Z., Y.L., J.V.L., M.L., V.P., M.E.Y., Z.S., Y.D., W.W., H.D., L.S., X.W., L.Le, X.F, H.G., R.A. and S.Y.W. performed experiments. W.X., D.G., M.Y. and M.G. analysed the data. J.G., S.M., D.J., T.D.N. and Z.L. performed pig cloning and generated pigs. J.M., W.Q. and W.F.W. revised the manuscript.

Competing interests

Y.Y., W.X., Y.Z., X.S., M.Y., J.W., J.X., M.X., Q.Z., Y.L., H.D., L.S., X.W., L.Le, X.F., Y.G. and L.Y. are employed by Qihan Bio Inc. Y.K., D.G., L.Lamriben, J.V.L., M.L., V.P., M.E.Y., H.G., R.A., S.Y.W., W.F.W. and W.Q. are employed by eGenesis Inc. M.G. is a consultant to Qihan Bio Inc. and eGenesis Inc. J.M. is an advisor on the scientific advisory board of Qihan Bio Inc. and eGenesis Inc. G.M.C. is the cofounder and scientific advisor of Qihan Bio Inc. and eGenesis Inc. Y.K., M.G., W.Q., Y.G. and L.Y. are listed as inventors on a provisional patent application pertaining to the results of the paper.

Additional information

Supplementary information is available for this paper at https://doi.org/10.1038/s41551-020-00613-9.

Correspondence and requests for materials should be addressed to L.Y.

Reprints and permissions information is available at www.nature.com/reprints.

Publisher's note Springer Nature remains neutral with regard to jurisdictional claims in published maps and institutional affiliations.

nature research

Corresponding author(s): Luhan Yang

Last updated by author(s): Jun 19, 2020

Reporting Summary

Nature Research wishes to improve the reproducibility of the work that we publish. This form provides structure for consistency and transparency in reporting. For further information on Nature Research policies, see our Editorial Policies and the Editorial Policy Checklist.

Statistics

For all statistical analyses, confirm that the following items are present in the figure legend, table legend, main text, or Methods section.

n/a	Confirmed	
☐	☒	The exact sample size (*n*) for each experimental group/condition, given as a discrete number and unit of measurement
☐	☒	A statement on whether measurements were taken from distinct samples or whether the same sample was measured repeatedly
☐	☒	The statistical test(s) used AND whether they are one- or two-sided *Only common tests should be described solely by name; describe more complex techniques in the Methods section.*
☒	☐	A description of all covariates tested
☐	☒	A description of any assumptions or corrections, such as tests of normality and adjustment for multiple comparisons
☐	☒	A full description of the statistical parameters including central tendency (e.g. means) or other basic estimates (e.g. regression coefficient) AND variation (e.g. standard deviation) or associated estimates of uncertainty (e.g. confidence intervals)
☐	☒	For null hypothesis testing, the test statistic (e.g. *F*, *t*, *r*) with confidence intervals, effect sizes, degrees of freedom and *P* value noted *Give P values as exact values whenever suitable.*
☒	☐	For Bayesian analysis, information on the choice of priors and Markov chain Monte Carlo settings
☒	☐	For hierarchical and complex designs, identification of the appropriate level for tests and full reporting of outcomes
☒	☐	Estimates of effect sizes (e.g. Cohen's *d*, Pearson's *r*), indicating how they were calculated

Our web collection on statistics for biologists contains articles on many of the points above.

Software and code

Policy information about availability of computer code

Data collection	HTS data, images, and flow-cytometry data were collected with a standard Illumina sequencer, the Leica Fluorescence Microscope, and the Beckman CytoFLEX S flow cytometer (CytExpert 2.3), respectively.
Data analysis	FlowJo 10.6.2, ImageJ 1.52a with Java v1.8.0_112, BWA v0.7.17-r1188, GATK v4.0.7.0, CRISPRSeek v1.22.1, R v3.5.0, VEP v93.3, STAR 2.6.1a, Salmon v0.11.3, Picard v2.8.14, EXCEL v2016.

For manuscripts utilizing custom algorithms or software that are central to the research but not yet described in published literature, software must be made available to editors and reviewers. We strongly encourage code deposition in a community repository (e.g. GitHub). See the Nature Research guidelines for submitting code & software for further information.

Data

Policy information about availability of data

All manuscripts must include a data availability statement. This statement should provide the following information, where applicable:

- Accession codes, unique identifiers, or web links for publicly available datasets
- A list of figures that have associated raw data
- A description of any restrictions on data availability

The main data supporting the findings of this study are available within the paper and its Supplementary Information. Data from the RNA-seq analyses are available in figshare with the identifier doi.org/10.6084/m9.figshare.12841418.v1. The raw data generated during the study are available at the China National GeneBank, with the accession string CNP0001254. The pig reference genome (Sus scrofa 11.1) sequence was obtained from Ensembl, ftp://ftp.ensembl.org/pub/release-91/fasta/sus_scrofa/dna. The pig transcript isoform information was obtained from the APPRIS database, http://appris.bioinfo.cnio.es/#/seeker.

Field-specific reporting

Please select the one below that is the best fit for your research. If you are not sure, read the appropriate sections before making your selection.

☒ Life sciences ☐ Behavioural & social sciences ☐ Ecological, evolutionary & environmental sciences

For a reference copy of the document with all sections, see nature.com/documents/nr-reporting-summary-flat.pdf

Life sciences study design

All studies must disclose on these points even when the disclosure is negative.

Sample size	No statistical methods were used to predetermine sample size. We analysed all data available.
Data exclusions	No data were excluded from the analyses.
Replication	Independent replicates are all reported. All attempts at reproducibility succeeded, as defined by (at a minimum) two or three positive results.
Randomization	Samples were not randomized.
Blinding	The investigators were not blinded to group allocation.

Reporting for specific materials, systems and methods

We require information from authors about some types of materials, experimental systems and methods used in many studies. Here, indicate whether each material, system or method listed is relevant to your study. If you are not sure if a list item applies to your research, read the appropriate section before selecting a response.

Materials & experimental systems

n/a	Involved in the study
☐	☒ Antibodies
☐	☒ Eukaryotic cell lines
☒	☐ Palaeontology and archaeology
☐	☒ Animals and other organisms
☐	☒ Human research participants
☒	☐ Clinical data
☒	☐ Dual use research of concern

Methods

n/a	Involved in the study
☒	☐ ChIP-seq
☐	☒ Flow cytometry
☒	☐ MRI-based neuroimaging

Antibodies

Antibodies used	We have listed all the antibodies used in Supplementary Table 2 alongside supplier name, catalog number, clone name and lot number.
Validation	All antibodies were validated.

Eukaryotic cell lines

Policy information about cell lines

Cell line source(s)	Human umbilical vein endothelial cells (HUVECs), human NK-92 cell line and human THP-1 macrophage cell lines were obtained from ATCC. Porcine fetal fibroblast cells, ear fibroblast cells and porcine umbilical vein endothelial cells (PUVECs) were isolated from 3KO·9TG pigs or PERVKO·3KO·9TG pigs.
Authentication	HUVECs were validated by staining with anti-human CD31 antibody. Porcine umbilical vein endothelial cells were validated by staining with anti-pig CD31 antibody. THP-1 cells were validated by being differentiated into macrophages, which were further validated by staining with anti-human CD11b antibody.
Mycoplasma contamination	All cells initially tested negative for mycoplasma by the manufacturer. Cells were periodically tested during experimentation. No mycoplasma contamination was found.
Commonly misidentified lines (See ICLAC register)	No commonly misidentified cell lines were used.

Animals and other organisms

Policy information about studies involving animals; ARRIVE guidelines recommended for reporting animal research

Laboratory animals	Crossbred (Large White/Landrace/Duroc) sows (7 months – 1.5 years, female) and cloned Bama pigs (2 days – 2 years, male) were used in this study.
Wild animals	The study did not involve wild animals.
Field-collected samples	The study did not involve samples collected from the field.
Ethics oversight	The Animal Care Committee of Yunnan Agricultural University, China, approved the animal-study protocols.

Note that full information on the approval of the study protocol must also be provided in the manuscript.

Human research participants

Policy information about studies involving human research participants

Population characteristics	The donors were checked before drawing blood, to ensure that they were generally healthy.
Recruitment	Enrollment was based on voluntary participation. No selection biases were present.
Ethics oversight	The study was approved by the human research ethics committee, Second Affiliated Hospital, Zhejiang University School of Medicine

Note that full information on the approval of the study protocol must also be provided in the manuscript.

Flow Cytometry

Plots

Confirm that:

☒ The axis labels state the marker and fluorochrome used (e.g. CD4-FITC).

☒ The axis scales are clearly visible. Include numbers along axes only for bottom left plot of group (a 'group' is an analysis of identical markers).

☒ All plots are contour plots with outliers or pseudocolor plots.

☒ A numerical value for number of cells or percentage (with statistics) is provided.

Methodology

Sample preparation	Validation of genetic modification at protein level by FACS: Cells were harvested, fixed and then stained using corresponding primary and secondary antibodies (Supplementary Table 2), according to the manufacturer's instructions. Isotype controls were applied at the same final dilution as the specific primary antibodies. After antibody staining, cells were washed twice, and analysed by FACS using a CytoFLEX S flow cytometer.
Instrument	Beckman CytoFLEX S flow cytometer and SONY SH800S cell sorter.
Software	Data were collected using Beckman CytExpert 2.3 (the software used by CytoFLEX S flow cytometer) and analysed using FlowJo 10.6.2 Software tools used for NGS data analysis are listed in Methods.
Cell population abundance	Nine days after transfection, 3KO·9TG cells that are negative for GGTA1 and positive for both CD46 and CD39 were sorted into 96-well plates by using a SONY SH800S cell sorter. The GGTA1-CD46+CD39+ populations are approximately 6% of the population and were sorted as single cells into 96-well plates according to the supplier's protocol.
Gating strategy	Debris was gated out using SSC-A vs. FSC-A graph. SSC-H vs. SSC-A graphs were used to select single events. All the gating strategies used in this work are included in Supplementary Figs. 10, 15 and 16.

☒ Tick this box to confirm that a figure exemplifying the gating strategy is provided in the Supplementary Information.